ARTICLES

Time-Resolved CARS of the Vibron Line Shape of Crystalline Nitrogen at Low Temperature and High Pressure

Bruce J. Baer and Eric L. Chronister*

Department of Chemistry, University of California, Riverside, California 92521

Received: January 16, 1997; In Final Form: June 10, 1997[⊗]

Temperature- and pressure-dependent vibrational dephasing results for the alpha, gamma, and epsilon phases of crystalline nitrogen are obtained by time-resolved CARS measurements at high pressure (0−36 kbar) and low temperature (5−35 K). The very small homogeneous contribution to the vibrational line width in crystalline nitrogen at low temperature leads to vibronic dephasing that is dominated by weak inhomogeneous effects. Specifically, crystalline nitrogen cannot be cooled to low temperature without experiencing polymorphic solid-state phase transitions. For example, the β-$N_2 \rightarrow$ α-N_2 phase transition at ambient pressure, or the β-$N_2 \rightarrow$ γ-N_2 transition between 4 and 21 kbar, may generate defects leading to an inhomogeneous distribution of vibronic site energies. In each case, crystalline β-N_2 is formed starting from the supercritical fluid, by either cooling or compression. The negligible homogeneous contribution to the vibron line width for nitrogen at low temperature (<10 K) allows one to probe details of the extremely small inhomogeneous contributions to the vibron line shape. At higher temperature the vibronic dephasing rate increases and is analyzed in terms of a dominant quartic dephasing process involving thermally populated optical phonons.

Introduction

There have been several studies of the vibronic line width of the alpha crystalline phase of solid nitrogen at ambient pressure.[1−6] Two earlier time-resolved CARS studies of α-N_2 have reported seemingly inconsistent results, due to the different time scales and dynamic ranges of the two studies.[3−5] Time-resolved stimulated Raman scattering experiments by Abram and Hochstrasser[3] used 6 ns pulses and measured coherence decays out to 100 ns over 7 orders of magnitude in CARS intensity. The relatively weak intensity at long times was found to decay as $\exp(-(t/\tau)^{1/2})$.[7] In contrast, a subsequent time-resolved CARS study by DeKinder et al.[5] using 6 ps pulses, a time window of 1.2 ns, and a dynamic range of 2 orders of magnitude yielded coherence decays that were fit by the product of an exponential and a Gaussian. Since the entire time scale of the CARS decay window of DeKinder et al.[5] was within the excitation pulse width of the previous experiment,[7] a direct comparison of the experimental results is precluded. Due to the faster time resolution (7 ps) and broader laser bandwidth (8 cm^{-1}) utilized in the latter study, DeKinder et al. were also able to observe the beat pattern due to the $\sim$1 cm^{-1} splitting of the A_g and T_g modes of the alpha phase.[5] However, inhomogeneous broadening clearly dominated the CARS decays within the 1.2 ns time window of DeKinder et al. and was attributed to a statistical distribution of crystal defects. Scattering by isotopic impurities was discounted since the dephasing time was unaffected by an increase in the ^{15}N concentration.[3−4]

The vibrational lifetime of N_2 is expected to be unusually long at low temperature, relative to other condensed phase molecular systems,[8−9] due to the high-order phonon emission processes needed to conserve energy. Although the vibronic lifetime of crystalline N_2 has not been reported, the vibrational lifetime reported for O_2 in solid Ar at low temperature is estimated to be $\sim$1650 s,[10] while the vibrational lifetime in liquid N_2 at 1 atm and 77 K has been reported to be 56 ± 10 s.[11] These systems illustrate the slow vibrational relaxation rate associated with a very high order relaxation process. Thus, the low-temperature Raman line shape of crystalline N_2 can be dominated by small inhomogeneous effects. Although time-resolved CARS yields the total vibrational dephasing time (including inhomogeneous effects), other spectroscopic techniques such as Raman echo[12] or infrared vibrational photon echo[13,14] can be utilized to separate inhomogeneous spectral broadening effects.

At pressures below 4 GPa there are three low-temperature crystalline phases of nitrogen, denoted α-, γ-, and ϵ-N_2, in order of increasing pressure.[15−16] The ambient pressure phase of nitrogen, α-N_2, is cubic (space group $Pa3$) with 4 molecules per unit cell[17] and has vibrationally active Raman modes of A_g and T_g symmetry (with a splitting $\sim$1 cm^{-1}). The γ-N_2 crystalline phase exists over the pressure range 3.5−21 kbar at low temperature, is tetragonal (Space group $P4_2/mnm$), with two molecules per unit cell, and has two vibrationally active Raman modes of A_{1g} and B_{2g} symmetry (with a reported splitting of 1.5 cm^{-1}).[16,18−19] The ϵ-N_2 crystalline phase exists above 20 kbar (up to $\sim$200 kbar), is rhombohedral (space group $R\bar{3}c$),[20] with eight molecules per unit cell, and has two vibrationally active Raman modes of A_{1g} and E_g symmetry (with a splitting of 6 cm^{-1} at 20 kbar, increasing to 25 cm^{-1} at 200 kbar).[16] The phase diagram for N_2 has been well documented in these pressure−temperature ranges.[15,16,19,20]

Given the large energy mismatch between the $\sim$2330 cm^{-1} intramolecular vibron frequency of nitrogen and the highest frequency intermolecular phonon mode, cubic relaxation and dephasing processes other than intraband scattering are precluded, even at elevated temperature. Although pressure-

* To whom correspondence should be addressed. Fax: (909) 787-4713. Email: eric.chronister@ucr.edu.

[⊗] Abstract published in *Advance ACS Abstracts,* September 1, 1997.

S1089-5639(97)00237-5 CCC: $14.00

induced expansion of the phonon spectrum can in general open new vibronic relaxation pathways,[21] in nitrogen the energy gap is so large that small inhomogeneous contributions to vibronic line width are expected to dominate the low temperature line width even at high pressure. At higher temperatures (e.g. >15 K), thermally induced homogeneous dephasing contributes to the vibrational line width of crystalline N_2.[1,2,4,22] However, given the large energy gap between the vibron energy and the phonon band, a quartic dephasing process is the lowest order dephasing mechanism possible at elevated temperature. A computational study of vibrational dephasing in solid N_2 has reported that thermally induced quartic dephasing is dominant.[22] Therefore, the psCARS results from 5 to 35 K are analyzed in terms of quartic dephasing processes involving a thermally populated optical phonon.

The present picosecond CARS study reports vibronic dephasing results on a time scale intermediate to that of ref 3 and refs 4 and 5 in order to investigate the nature of the inhomogeneous effects that dominate the vibronic dephasing at low temperature. The negligible homogeneous contribution to the vibron line width for nitrogen at low temperature allows one to probe extremely small inhomogeneous contributions to the vibron line shape. In addition, since crystalline nitrogen cannot be cooled to low temperature without experiencing a polymorphic solid-state phase transition (e.g. β-$N_2 \rightarrow \alpha$-N_2 at ambient pressure, or β-$N_2 \rightarrow \gamma$-N_2 at pressures between 4 and 21 kbar) we also compare low-temperature psCARS results for α-,[17] γ-,[18,19] and ϵ-N_2[20] to investigate the effect of different polymorphic phase transitions on the vibronic dynamics.

Experimental Section

Samples were prepared by loading liquid nitrogen into the 400 μm aperture of an inconel gasket in a diamond anvil cell of the Merrill−Bassett design[23] using the immersion technique.[24] The load was performed inside a nitrogen-purged glovebox to minimize contamination by air. This procedure should yield a sample purity comparable to our source liquid nitrogen (>99.9% based upon normal boiling point). The sample aperture also contained small ruby chips as a pressure gauge.[25] The uncertainty in pressure for our system is ∼0.6 kbar, determined by the ruby luminescence.

Low temperatures were achieved through the use of a Janis Supertran VP System continuous helium flow cryostat. Temperatures between 4.3 and 40 K were achieved by varying the helium flow plus the use of a temperature controlled heater. Data were typically collected every 5 K from 5 to 35 K with an accuracy of <0.2 K. Cooling a nitrogen sample from ambient temperature to 15 K typically resulted in a pressure drop of 6−8 kbar, due to the volume change associated with each phase transition.

Time-resolved CARS measurements were obtained using laser pulses at 532 and 607 nm. A mode-locked and Q-switched Nd:YAG laser was frequency doubled to generate 532 nm pulses which synchronously pumped a cavity-dumped dye laser (rhodamine 640 in methanol). A Pockels cell was used to select a single 532 nm pulse which was split in two with a dielectric beamsplitter. One of the 532 nm pulses was temporally and spatially overlapped with the 607 nm dye laser pulse, while the other 532 nm probe pulse was time delayed. An intracavity etalon in the dye laser yielded a bandwidth of ∼1 cm^{-1}, and the instrument response time for the psCARS decays was ∼30 ps. CARS emission was spatially and spectrally filtered, detected with a photomultiplier tube, digitized (12 bit A/D), and analyzed by computer. A computer-controlled stepper motor variable delay line was used to obtain the CARS intensity as a function of probe pulse delay. This system's dynamic range is about 3 orders of magnitude and the optical delay line yielded a time window of 4 ns. A spectrograph (Instruments SA HR320) with a CCD detector was used to distinguish between the two vibrons of ϵ-N_2, and was used to obtain ruby luminescence data for pressure determination.

Motional Narrowing of Inhomogeneously Broadened Vibrational Lines. A vibrational mode weakly coupled to a bath of other modes can be modeled as an oscillator with a time-dependent frequency shift.[26,27] Motional narrowing of the inhomogeneous line shape is expected when the intermolecular interaction energy β is greater than the variance of the Gaussian distribution of vibrational site energy fluctuations Δ, i.e., $\beta > \Delta$, resulting in a motionally narrowed Lorentzian line width contribution[26,27]

$$\Gamma \approx \Delta^2/\beta \tag{1}$$

Conversely, when the variance of the inhomogeneous distribution of site energies is greater than the intermolecular interaction energy, then a Gaussian line shape of width Δ is obtained. In intermediate cases where $\Delta \sim \beta$, the line shape is more complicated, but the convolution of a Lorentzian and a Gaussian line shape, i.e., a Voight line shape, is a useful phenomenological line shape function.[28]

For α-N_2 (with 4 molecules per unit cell) the $k = 0$ Raman-allowed A_g and T_g modes lie at the upper and lower edges of the vibron band with a ∼1.0 cm^{-1} splitting.[3,4] In addition, the magnitude of the variance in the distribution of site energies is estimated to be in the range 0.05−0.3 cm^{-1}.[3,7] Since the observed coherence decay times are much longer than the vibron residence time of ∼20 ps, some motional narrowing is expected in this system.

In the simplified treatment above, we have purposefully neglected the fact that vibron states can lie at critical points in the Brillouin zone with zero group velocity and that such states are expected to have more complicated line shapes.[7] The variability in the psCARS decays for high-pressure nitrogen crystals precludes such a detailed analysis of the line shape at this time. Since the time domain analogue of the Voight line shape given in eq 2 is simply the product of an exponential and a Gaussian decay function, it is a particularly useful line shape with which to characterize time-resolved dephasing measurements.

Results and Discussion

Polymorphic Phase Transitions. Crystalline nitrogen cannot be cooled to low temperature without traversing a polymorphic solid-state phase transition. Although β-N_2 is formed from the supercritical fluid by cooling or compression, further cooling at ambient pressure results in a polymorphic phase transition from β-N_2 to α-N_2, whereas a transition from β-N_2 to γ-N_2 occurs upon cooling at higher pressure (i.e., between 4 and 21 kbar). Since both β-N_2 and δ-N_2 are plastic crystals (exhibiting orientational disorder), the solid-state transition to an ordered crystalline phase (e.g. α-N_2, ϵ-N_2) upon cooling can introduce sample-dependent inhomogeneous broadening, due to orientational disorder frozen into the low-temperature phase.[29] The very small homogeneous contribution to the N_2 vibron line width at low temperature allows one to probe extremely small inhomogeneous contributions to the vibron line shape.

Low-Pressure α-N_2. For the alpha phase of N_2, we observed two types of CARS decays. Some samples exhibited a significant Gaussian component in the CARS decay (similar to

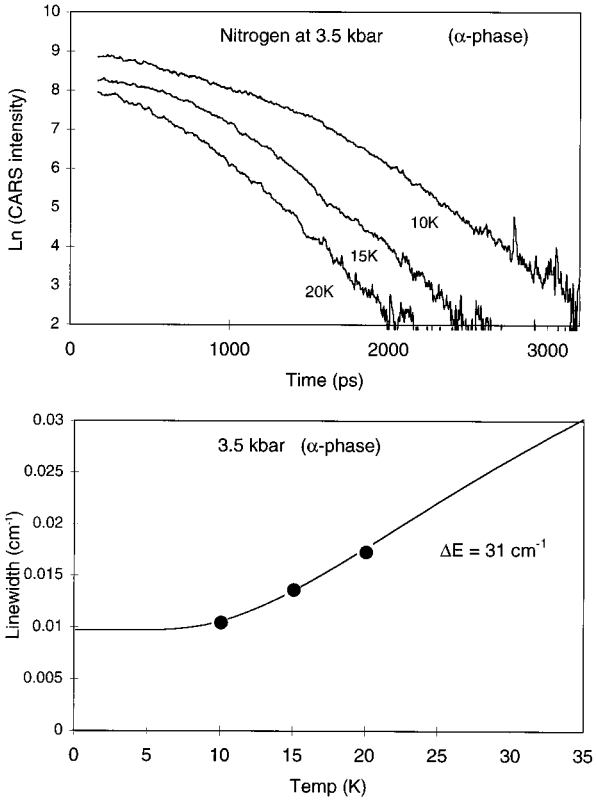

Figure 1. (top) A characteristic series of semilog plots of Gaussian-broadened time-resolved CARS decays for a sample α-N_2 at 3.5 ± 0.5 kbar. The solid curve is a fit of eq 4 to the temperature-dependent line widths obtained from the CARS data.

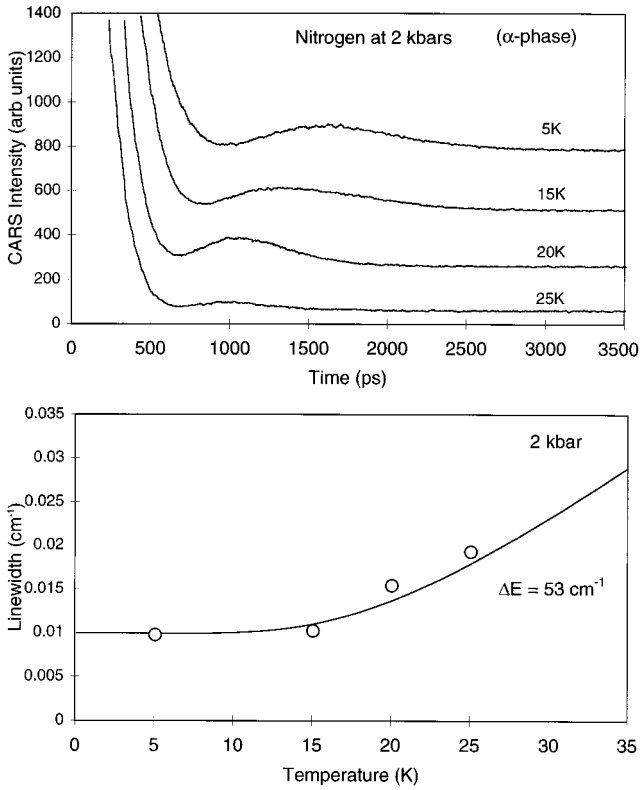

Figure 2. (top) A characteristic series of oscillatory CARS decays obtained for a sample of α-N_2 at 2.0 ± 0.5 kbar. The low-temperature CARS data was fit by eq 3, yielding two Lorentzian lines of line widths $T_2(1) = 0.007$ cm^{-1} and $T_2(2) = 0.018$ cm^{-1} split in frequency by $\Delta\nu = 0.014$ cm^{-1}. (bottom) The solid curve is a fit of eq 4 to the temperature-dependent line width of the narrower Lorentzian line obtained by fitting the CARS data to eq 3.

DeKinder et al.[5]), as shown in Figure 1, whereas some samples yielded a weak beat pattern in the CARS emission, as shown in Figure 2.

The CARS decays shown in Figure 1 were fit to the product of a Lorentzian and a Gaussian decay (i.e., a Voight line shape),

$$I_{\mathrm{CARS}} = I_0 \exp\left(-\frac{2t}{T_2} - \frac{\ln 2 \cdot t^2}{\tau_G^{\,2}}\right) \qquad (2)$$

where T_2 is the homogeneous dephasing time and t_G is the half-maximum time for the Gaussian component of the CARS decay. The relative magnitudes of the Gaussian and Lorentzian contributions were found to vary from sample to sample.

The decaying CARS intensity oscillations in Figure 2 have a period of 1−2 ns, which we attribute to a splitting of one of the vibrons of α-N_2.[5] Since the Gaussian line width contributions were small, the oscillatory CARS decays in Figure 2 were modeled by two narrowly spaced Lorentzian lines, with a corresponding CARS intensity decay:

$$I_{\mathrm{CARS}} = A_i^{\,2} \exp\left(\frac{-2t}{T_2^{(1)}}\right) + A_2^{\,2} \exp\left(\frac{-2t}{T_2^{(2)}}\right) + 2A_1A_2 \exp\left[-t\left(\frac{1}{T_2^{(1)}} + \frac{1}{T_2^{(2)}}\right)\right] \cos(\Delta\nu t) \qquad (3)$$

where $T_2^{(1)}$ and $T_2^{(2)}$ represent the dephasing times of two Lorentzian lines of amplitude A_1 and A_2 with a frequency splitting of $\Delta\nu = \nu_1 - \nu_2$. By fitting the data in Figure 2 (top panel) to eq 3 we obtain the temperature-dependent line width, $\Gamma = (\pi c T_2)^{-1}$, which is shown for the narrower Lorentzian line in the bottom panel of Figure 2.

The large energy mismatch between the ∼2330 cm^{-1} intramolecular N_2 vibron frequency and the intermolecular phonon frequencies precludes cubic relaxation and/or dephasing processes that cannot conserve energy (other than intraband scattering). Intraband scattering involving coupling to acoustic phonons is not expected to be significant due to the small acoustic density of states below 1 cm^{-1}. However, at higher temperatures the simultaneous absorption and emission of optical phonons can dephase the optically excited vibron by quartic and higher order dephasing mechanisms.

A computational study of vibrational dephasing in crystalline nitrogen indicates that the dominant thermally induced dephasing mechanisms are quartic processes.[22] Thermal occupation of phonon modes involved in the quartic dephasing process leads to an increase in the dephasing rate. For a quartic process involving the creation and annihilation of a phonon, p, the dephasing rate is proportional to $(n_p + 1)(n_p)$ which reduces to eq 4 in the low-temperature limit ($kT \ll h\nu_{\mathrm{phonon}}$, $n_p \ll 1$).

$$\Gamma = \Gamma_0 + b \exp(-h\nu_{\mathrm{phonon}}/kT) \qquad (4)$$

where Γ_0 is the intrinsic line width and $h\nu_{\mathrm{phonon}}$ represents a phonon activation energy. The solid curve in Figure 2 (bottom) is a fit of the data to eq 4, yielding $\nu_{\mathrm{phonon}} = 53$ cm^{-1} for α-N_2 at 2 kbar. Although motional narrowing of the inhomogeneous broadening can yield Lorentzian line shapes at low temperature, at elevated temperatures, thermally induced quartic dephasing processes can give rise to homogeneous line broadening. The fit of eq 4 to the data in the lower panel of Figure 1 yields a phonon energy of $\nu_{\mathrm{phonon}} = 31$ cm^{-1} for the thermally induced homogeneous dephasing in a Gaussian broadened α-N_2 sample at 3.5 kbar. In general, Gaussian-broadened lines tended to have lower phonon activation energies than corresponding Lorentzian-broadened lines at a similar pressure. This result may indicate

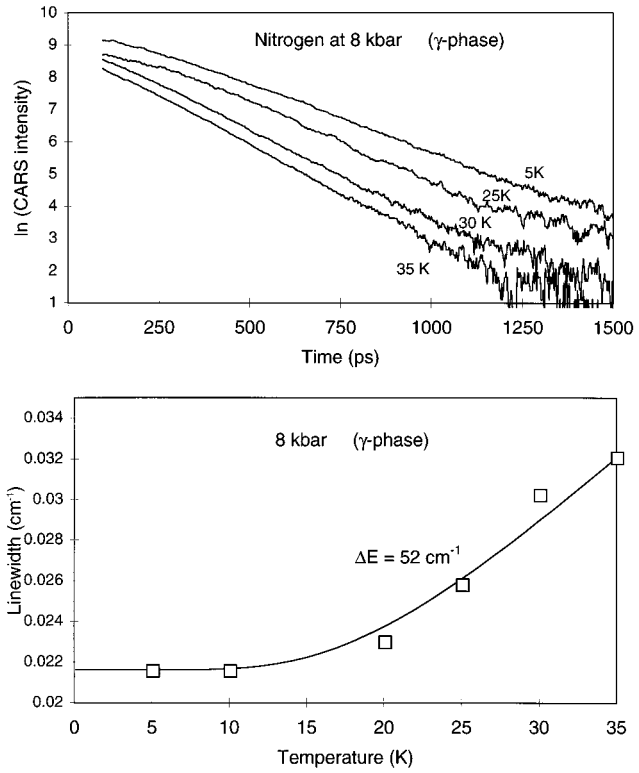

Figure 3. (top) Typical semilog plot of the exponential CARS decays observed for samples of γ-N_2 at 8 ± 0.5 kbar. The solid line is a fit of eq 4 to the temperature-dependent line widths obtained from the CARS data.

that the breaking of translational symmetry (associated with inhomogeneous broadening) may allow dephasing mechanisms otherwise restricted by momentum conservation. The different temperature-dependent data observed in Figures 1 and 2 suggests that different inhomogeneous distributions contain different local environments with unique activated dephasing processes.

High-Pressure γ-N_2. Single-exponential psCARS decays were observed for the gamma phase of nitrogen (>3.5 kbar) at all temperatures, as shown in Figure 3. However, the magnitudes of the decay times in high-pressure γ-N_2 were dependent upon the preparation of the sample. Although most samples yielded CARS decay times of less than 150 ps at 15 K, decay times greater than 200 ps at 15 K were observed for some samples. In general, we tried to select samples with the longest decays times since these samples allowed for a greater dynamic range for temperature-dependent vibrational dephasing measurements. Samples with fast decay times at low temperature tended to show little temperature dependence over the 5−35 K temperature range, due to greater intrinsic inhomogeneous broadening. The fit of eq 4 to the temperature-induced line broadening in Figure 3 yields a phonon energy of $\nu_{phonon} = 52$ cm^{-1}. For a quartic homogeneous dephasing mechanism, this activation energy represents an average energy of thermally populated phonon modes involved in the dephasing of the intramolecular vibron at elevated temperatures.

Although previous spontaneous Raman experiments hint that the two Raman active vibrations of the gamma phase are discernible,[15] no indications of a beat pattern were present in our CARS data. The two modes are expected to have different polarized Raman spectra, but no CARS emission was detected when the polarizations of the 532 nm and the 607 nm excitation beams were set to probe the B_{2g} mode.

High-Pressure ϵ-N_2. We studied the vibrational dephasing of epsilon nitrogen from 21 to 36 kbar (not shown). Although motionally narrowed exponential CARS decays were obtained for ϵ-N_2, the resulting line widths ($\sim$0.08 cm^{-1} for samples with the narrowest line widths) were significantly broader than was observed for the lower pressure crystalline phases. Because of the large static inhomogeneous broadening contribution to the line width in high-pressure ϵ-N_2, the line width was observed to be independent of temperature below 35 K. When the samples were annealed at the $\gamma-\epsilon$ phase transition pressure of 21 kbar, a composite crystal of gamma and epsilon nitrogen was obtained which yielded a biexponential CARS decay.

Inhomogeneous Line Broadening in High-Oressure Crystals of N_2. The extremely long vibrational lifetimes observed for diatomic vibrations in low-temperature atomic matrices and for liquid N_2 at 77 K[11] suggests that the line width of anything except a perfect nitrogen crystal will be inhomogeneously broadened at low temperature. The narrowest vibrational line width observed in this study (e.g. $\sim$0.005 cm^{-1} in α-N_2) was most likely many orders of magnitude larger than the homogeneous relaxation contribution to the line width.

Although pressure-induced inhomogeneous broadening is minimal within a given phase, the higher pressure phases are increasingly dominated by inhomogeneous broadening, which suggests that the different polymorphic phase transitions are largely responsible for the resulting inhomogeneous width. A variety of crystal growth methods were evaluated to minimize spectral broadening, such as annealing at the phase transition temperature. Since inhomogeneous broadening in crystalline N_2 has been attributed to a statistical distribution of defects,[3,7] it appears that increased pressure increases the number of defects and that annealing processes (at the phase transition pressures) may be inhibited at higher pressure.

The $\sim$1 cm^{-1} bandwidth of the dye laser permitted selective excitation of the A_g and E_g modes of the epsilon phase, but not the A_g and T_g vibrons in the alpha phase. The CARS oscillations in Figure 2 correspond to a splitting of 0.014 cm^{-1}, which is much smaller than the 1.0 cm^{-1} A_g-T_g factor group splitting in α-N_2. Given the weak Raman intensity of the T_g mode, and the polarization conditions of the CARS emission, the CARS oscillations are attributed to a discrete splitting of the A_g vibron. Different microcrystallites within a given sample may have different distributions of defects depending on their pressure and temperature history (samples are pressurized at ambient temperature and subsequently cooled). Furthermore, twinning on the {111} planes in α-N_2 has been suggested from the observation of symmetry-forbidden diffraction peaks in the crystallographic determination of this phase.[17]

Although a variety of different vibrational dephasing dynamics are observed in different samples, the actual *magnitude* of the inhomogeneous line widths (and the changes) are rather small (e.g. <0.03 cm^{-1}). Even though the inhomogeneous line shape is found to be sample dependent, we have categorized the observed decays into three different types: (1) exponential decays, (2) Gaussian broadened decays, and (3) coherent beating between multiple exponential decay components. In crystalline nitrogen, the CARS dynamics are very sensitive to small changes in the inhomogeneous line shape since it dominates the coherence loss at low temperature.

Thermally Activated Dephasing. Figures 1−3 show temperature-induced vibrational dephasing at higher temperatures and Arrhenius fits yielded phonon activation energies for the vibrational dephasing. In the alpha phase we either observe CARS decays with a significant Gaussian component (Figure 1) or CARS oscillations that can be fit by a pair of Lorentzian spectral lines (Figure 2). The temperature dependence of the Gaussian-broadened α-N_2 decay in Figure 1 yielded a phonon frequency of $\nu_{phonon} = 31 \pm 6$ cm^{-1}, whereas the temperature

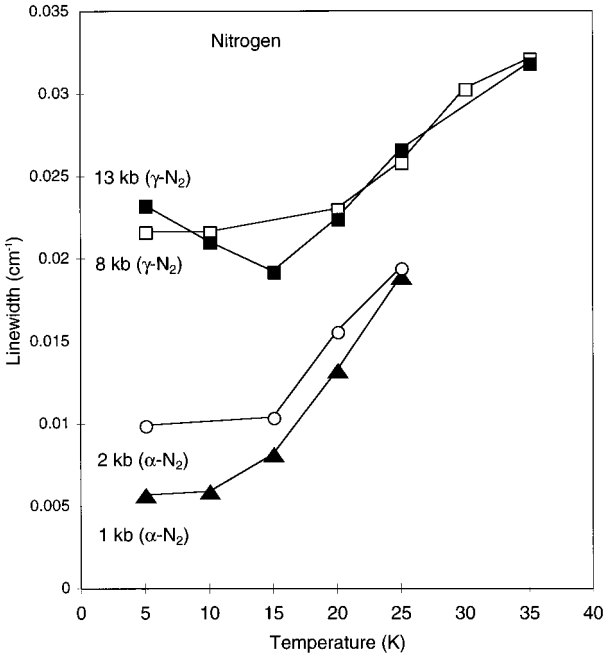

Figure 4. Line width vs temperature plot of selected samples in the alpha and gamma phase. The line widths at low temperature are completely dominated by inhomogeneous broadening. At higher temperatures, homogeneous quartic dephasing gives rise to line broadening.

dependence of one of the Lorentzian doublets in Figure 2 yielded $\nu_{\text{phonon}} = 53 \pm 6$ cm^{-1}. The thermal activation energies may be interpreted as the average phonon energies of the thermally populated phonon modes involved in the quartic dephasing mechanism of the vibron at elevated temperatures.

The fact that different ν_{phonon} values are obtained in Figures 1 and 2 suggests that a distribution of quartic processes may be involved. The different activation energies imply that changes in the local environment can affect the coupling strength to different phonon modes involved in the dephasing process. For the vibrational dephasing in the gamma phase, $\nu_{\text{phonon}} = 52 \pm 8$ cm^{-1} and this value is observed to increase with pressure to a value of 69 ± 8 cm^{-1} at 13 kbar (not shown). The pressure-induced phonon energy shifts observed for γ-N_2 are consistent with those observed in spontaneous Raman studies on this system.[16,30]

In α-N_2, Gaussian-broadened lines tended to have lower phonon activation energies than corresponding Lorentzian-broadened lines at a similar pressure, suggesting that broken translational symmetry (associated with inhomogeneous broadening) may relax momentum conservation restrictions. In ϵ-N_2 a comparatively large amount of inhomogeneous broadening dominated the dephasing, resulting in nearly temperature independent results over the (5−35 K) temperature range of this study.

For some of the high-pressure nitrogen crystals we observed a small decrease in the line width as the temperature was raised from 5 to 15 K. One example of this is illustrated by the 13 kbar γ-N_2 data in Figure 4. This effect may represent a temperature-dependent motional narrowing effect (since it occurs at a temperature where the inhomogeneous and homogeneous dephasing contributions are comparable), or alternatively, it may represent temperature-induced changes in inhomogeneous strain broadening.

Conclusions

The negligible homogeneous contribution to the vibron line width in crystalline N_2 at low temperature (<10 K) allows psCARS measurements to probe small inhomogeneous contributions to the vibron line shape. Inhomogeneous vibronic effects are found to be influenced by the different polymorphic solid-state phase transitions involved in forming high pressure α-, γ-, and ϵ-N_2 crystals at low temperature. Although it was not possible to reproduce specific sample strains or frozen orientational defects, the psCARS results were categorized into three distinct types of coherence decays.

At higher temperature the vibronic dephasing rate increased due to interactions of the vibron with thermally populated optical phonons. These results yielded phonon activation energies which are attributed to optical phonons involved in quartic dephasing processes of the N_2 vibron. In α-N_2 the phonon activation energy was correlated with the functional form of the Raman line shape, while in γ-N_2 the phonon activation energy increased with pressure similar to that observed for pressure-induced shifts in the optical phonon spectrum of the crystal.

Acknowledgment. We greatly appreciate financial support from the National Science Foundation (CHE-9400542) for this research.

References and Notes

(1) Ouillon, R.; Turc, C.; Lemaister, J.-P.; Ranson, P. *J. Chem. Phys.* **1990**, *93*, 3005.

(2) Beck, R. D.; Hineman, M. F.; Nibler, J. W. *J. Chem. Phys.* **1990**, *92*, 7068.

(3) Abram, I. I.; Hochstrasser, R. M.; Kohl, J. E.; Semack, M. G.; White, D. *J. Chem. Phys.* **1979**, *71*, 153.

(4) DeKinder, J.; Goovaerts, E.; Bouwen, A.; Schoemaker, D. *Phys. Rev. B* **1990**, *42*, 5953.

(5) DeKinder, J.; Goovaerts, E.; Bouwen, A.; Schoemaker, D. *J. Lumin.* **1990**, *45*, 423.

(6) Beck, R.; Nibler, J. W. *Chem. Phys. Lett.* **1989**, *159*, 79.

(7) Abram, I. I.; Hochstrasser, R. M. *J. Chem. Phys.* **1980**, *72*, 3617.

(8) Hesp, B. H.; Wiersma, D. A. *Chem. Phys. Lett.* **1980**, *75*, 423.

(9) Ho, F.; W.-S. Tsay, Trout, J.; Hochstrasser, R. M. *Chem. Phys. Lett.* **1981**, *83*, 5.

(10) Salloum, A.; Dubost, H. *Chem. Phys.* **1994**, *189*, 179−204.

(11) Brueck, S. R. J.; Osgood, R. M., Jr. *Chem. Phys. Lett.* **1976**, *39*, 568.

(12) Vanden Bout, D.; Berg, M. *J. Raman. Spectrosc.* **1995**, *26*, 503.

(13) Tokmakoff, A.; Zimdars, D.; Urdahl, R. S.; Francis, R. S.; Kwok, A. S.; Fayer, M. D. *J. Phys Chem.* **1995**, *99*, 13310.

(14) Tokmakoff, A.; Fayer, M. D. *Acc. Chem. Res.* **1995**, *28*, 437.

(15) Buchsbaum, S.; Mills, R. L.; Schiferl, D. *J. Phys. Chem.* **1984**, *88*, 2522.

(16) Schiferl, D.; Buchsbaum, S.; Mills, R. L. *J. Phys. Chem.* **1985**, *89*, 2324.

(17) Venables, J. A.; English, C. A. *Acta Crystallogr.* **1994**, *B30*, 929.

(18) Mills, R. L.; Schuch, A. F. *Phys. Rev. Lett.* **1969**, *20*, 1154.

(19) Schuch, A. F.; Mills, R. L. *J. Chem. Phys.* **1970**, *52*, 6000.

(20) Mills, R. L.; Olinger, B.; Cromer, D. T. *J. Chem. Phys.* **1986**, *84*, 2837.

(21) Chronister, E. L.; Crowell, R. A. *Mol. Cryst. Liq. Cryst.* **1992**, *211*, 361.

(22) Procacci, P.; Signorini, G. F.; Della Valle, R. G. *Phys. Rev. B* **1993**, *47*, 11124.

(23) Merrill, L.; Bassett, W. A. *Rev. Sci. Instrum.* **1974**, *45*, 290.

(24) Schiferl, D.; Cromer, D. T.; Mills, R. L. *High Temp.- High Press.* **1978**, *10*, 493.

(25) Forman, R.; Piermarini, G.; Barnett, J.; Block, S. *Science* **1972**, *176*, 284.

(26) Anderson, P. W. *J. Phys. Soc. Jpn.* **1954**, *9*, 316.

(27) Kubo, R. *Adv. Chem. Phys.* **1969**, *15*, 101.

(28) Debartolo, B. *Optical Interactions in Solids*; Wiley: New York, 1968; p 366.

(29) Kuchta, B.; Rohleder, K.; Etters, R.; Belak, J. *J. Chem. Phys.* **1995**, *102*, 3349−3353.

(30) Thiery, M. M.; Fabre, D.; Jean-Louis, M.; Vu, H. *J. Chem. Phys.* **1973**, *59*, 4559.